Journal of Thermal Biology 94 (2020) 102748

Contents lists available at ScienceDirect

Journal of Thermal Biology

journal homepage: http://www.elsevier.com/locate/jtherbio

Morphological response of the red palm weevil, *Rhynchophorus ferrugineus*, to a transient low temperature analyzed by computer tomography and holographic microscopy

Trinidad León-Quinto [a,b,*], Antonio Fimia [c], Roque Madrigal [c], Arturo Serna [d]

[a] Área de Zoología, Universidad Miguel Hernández, E3202-Elche, Alicante, Spain
[b] Instituto de Bioingeniería, Universidad Miguel Hernández, E3202-Elche, Alicante, Spain
[c] Departamento de Ciencia de Materiales, Universidad Miguel Hernández, E3202-Elche, Alicante, Spain
[d] Departamento de Física Aplicada, Universidad Miguel Hernández, E3202-Elche, Alicante, Spain

ARTICLE INFO

Keywords:
Rhynchophorus ferrugineus
Insects
Global climate change
X-ray computer tomography
Digital holographic microscopy
Cryoprotectant
Glucose
Integument
Roughness
Cold hardiness

ABSTRACT

The red palm weevil (RPW), *Rhynchophorus ferrugineus*, is one of the worst palm pests worldwide. Our study aims to assess its internal and external morphological response to a sudden but transient decrease in the environmental temperature. Wild pre-pupae were subjected for 7 days to either low (5.0 ± 0.5 °C) or ambient temperature (23 ± 1 °C). Such conditions mimic a thermal anomaly happening in the larval stage most exposed to environmental factors. We quantified the changes undergone at: 1) the internal morphology, by X-Ray Computer Tomography (CT); 2) the 3-D integument' architecture, by Digital Holographic Microscopy (DHM); and 3) the glucose in hemolymph as a potential endogenous cryoprotectant. From X-ray CT we found that both pre-pupae subjected to cold and those remaining at ambient temperature follow a development where their fat body content decreases while a thick and dense cuticle is formed. There was no difference between both groups in the rate of change of fat body/dense tissues. Nevertheless, the cold group presents a slight developmental delay at the level of hemolymph content. Through DHM we again obtained that pre-pupae subjected to cold have not experienced a stop in their development. However, a more obvious developmental delay is now observed in this group at the level of the integumental roughness. Finally, regarding glucose, we found similar levels in control and ambient temperature larvae, while it was clearly increased in 51,7% of those subjected to cold. Our whole results provide morphological and biochemical evidence showing that the larval-pupal transition of the RPW continues almost undisturbed even during the quiescent state induced by a sudden and severe cold event. Nevertheless, a certain developmental delay is observed in both internal and external morphology. Additionally, the increased glucose level only found in the cold group suggests that glucose is part of the RPW cold tolerance strategy.

1. Introduction

Insects have developed a complex of strategies to survive low environmental temperatures. These strategies comprise (a) morphological, (b) behavioral, (c) ecological, (d) physiological and biochemical (freezing tolerance and freezing avoidance) adaptations (Lencioni, 2004). Most species develop a combination of these survival strategies, with high variation from one species to another. Indeed, some authors (e.g., Toxopeus and Sinclair, 2018) have emphasized that there is no specific strategy or class of molecule acting as a necessary ingredient for all cold-resistant insects. Each species requires its own study and, even for a given species, cold resistance may sometimes depend on several factors (Koštál et al., 2016; Denlinger and Lee, 2010).

Most studies on insect cold hardiness involve native species from cold areas (e.g., Saeidi and Moharramipour, 2017; Shao et al., 2018; Cubillos et al., 2018). The different responses to low temperatures of insects inhabiting warm geographical areas remain instead poorly known. In this paper we will focus on the red palm weevil (RPW), *Rhynchophorus ferrugineus* Olivier (Coleoptera: Dryophthoridae), which is considered to be one of the most destructive palm pests in warm areas worldwide. It is native to Southeast Asia and Oceania. However, because of the movement of live infested palms in recent decades, RPW has widely expanded to other regions of Asia, the Middle East, the Mediterranean Basin, Caribbean and California (Rugman-Jones et al., 2013),

* Corresponding author. Área de Zoología, Universidad Miguel Hernández, E3202-Elche, Alicante, Spain.
E-mail address: trini.leon@umh.es (T. León-Quinto).

https://doi.org/10.1016/j.jtherbio.2020.102748
Received 4 July 2020; Received in revised form 3 September 2020; Accepted 5 October 2020
Available online 7 October 2020

giving rise to huge environmental and economic losses.

Understanding how low temperature affects fitness of RPW is important for pest management, but also to deepen the knowledge of cold adaptation in insects from warm areas, especially in a context of unpredictable temperature variations linked to global climate change. Indeed, unseasonal cold or warm periods and events of extreme thermal anomalies are more and more frequent (Stouffer and Wetherald, 2007; Hansen et al., 2012, Bathiany et al., 2018), becoming a serious challenge for terrestrial ecosystems (Gu et al., 2008, Valenzuela et al., 2019).

Previous studies have analyzed the influence on RPW's life cycle of low temperatures (e.g., Martin and Cabello, 2005, 2006; Cabello, 2006). These studies found that prepupal and pupal stages are the most resistant to cold, with a lethal (0% survival) low temperature of 0 °C. Above this threshold, the survival rate depends on both temperature and exposure time. Lethal and optimal temperatures are then well established for the RPW. However, the cold survival strategy adopted by this species, native to warm geographic areas, remains poorly known at the morphological, physiological and biochemical levels.

In this paper, we will analyze the internal and external morphological response of the RPW to a sudden but transient decrease in the environmental temperature. Morphological changes are in fact among the main responses to environmental drivers (Gutiérrez et al., 2018). In many insects, this response mainly consists of a dormant state in which development temporarily stops or slows down (Nation, 2008; Gullan and Cranston, 2010). A form of this dormant state is quiescence that, in contrast to programmed or seasonal diapause, arises as an immediate response to unfavorable environmental conditions and ends when optimal conditions return. With some exceptions (Durak et al., 2020), most insects arrest their development during dormancy (e.g. Koštál et al., 2016; 2017). Here, we will compare the larval-pupal transition of prepupae subjected to a sudden cold stress with that observed in those remaining in favorable temperature conditions. Our aim will be to analyze whether the morphological response to cold stress consists of a cessation or delay in the development or RPW pre-pupae. We chose to focus on pre-pupae because, in wild conditions, this is the larval stage most exposed to the thermal characteristics of the environment. Indeed, the weevil spends most of its time inside the palm tree. However, mature grubs go to the periphery of the stem and prepare a cocoon made of palm fibers before entering the pupal stage (Dembilio and Jacas, 2011).

Until recently, the study of internal morphology required the use of destructive techniques such as dissection and microscopy. However, modern imaging techniques such as X-ray computed tomography (X-ray CT) allow the study of the internal whole animal in a non-destructive way, which in turn allows the analysis of internal traits before and after exposure to a specific stressor. In addition, images obtained from this technique possess a homogenous illumination with isotropic resolution at each slice, which allows consistent and precise volumetric estimates (Smith et al., 2016). In this work, we will use X-ray CT to quantify for the first time internal morphology changes happening in different tissues as fat body or hemolymph among others.

Concerning external morphology, such as the outermost layer of the integumentary system, conventional optical microscopy techniques such as phase contrast and differential interference contrast are well suited to observe qualitative structural and morphological changes. However, these techniques are often inadequate for the quantitative study of the three-dimensional (3-D) architecture. Digital holographic microscopy (DHM) is an imaging technology that is experiencing a tremendous growth and has potential applications in a wide range of areas including cellular microscopy, medical imaging, biometry, and environmental research (Kim, 2011). DHM is a technique that allows recording a hologram containing all the information necessary to reconstruct the 3-D architecture and quantify parameters such as surface roughness.

In order to have some insight on the biochemical aspects underlying the observed morphological response and the cold resistance strategy adopted by this species, we have also analyzed glucose as a possible endogenous cryoprotectant. Most overwintering insects accumulate high concentration of low molecular weight substances, such as sugars (e.g., glucose and trehalose), polyols (e.g., glycerol) and amino acids (e.g., proline), to promote cold hardiness and increase winter survival (Storey and Storey, 1988; Saeidi and Moharramipour, 2017; Toxopeus et al., 2019). Sugars act as stabilizers of the cell membranes protecting them from phase transition or freezing dehydration (Storey, 1997). Among other substances playing a cryoprotectant role in insects, an increase in glucose level has been reported in species living in cold zones (Saeidi and Moharramipour, 2017; Shao et al., 2018; Cubillos et al., 2018) and particularly in tropical species and non-seasonal cold events (Michaud and Denlinger, 2007; Overgaard et al., 2007, Wang et al., 2010; Teets and Delinger, 2013, Chowanski et al. 2015).

On the whole, in this paper we will carry out for the first time a quantitative analysis of how a sudden decrease in temperature affects: a) the development of the RPW main morphological components; b) the 3-D integument shape' architecture and c) the glucose level as a potential endogenous cryoprotective agent.

Knowing such responses could be relevant not only to deepen the knowledge of cold adaptation in insects inhabiting warm geographical areas, but also to drive the development of more effective management approaches.

2. Materials and methods

2.1. Insect sampling

Wild RPW larvae were collected in spring and autumn 2019 from infested palms, *Phoenix canariensis and Phoenix dactylifera*, located in the palm grove of Elche, Spain, a UNESCO World Heritage Site. Larval removal was carried out by qualified staff from TRAGSA, the public company that carries out the conservation of this palm grove. After collection, larvae were immediately taken to the laboratory, where we selected those in a wandering or prepupal stage. We then divided the selected animals into three groups:

a) *Control group*: formed by individuals immediately after their removal from their natural environment. All these individuals have fed on palm trees in wild conditions and underwent the different experiments the same day of their arrival at the laboratory.

b) *Cold treatment group*: formed by individuals placed for seven days in a climate chamber at low-temperature conditions (5.0 ± 0.5 °C). These individuals entered into a state of quiescence, where they remained until they returned to warm temperatures.

c) *No treatment (ambient temperature, AT) group*: formed by individuals that remained for seven days in a room under controlled ambient temperature (23 ± 1 °C). This temperature corresponds to the average found in autumn and spring for the periphery of the palm tree stems in the southeast of Spain (Dembilio and Jacas, 2011). Individuals in this group generally had a behavior of feeding cessation, very likely due to their wandering-prepupal stage. In order to homogenize the conditions of this group, all its individuals were subjected to starvation. Since cold-treated individuals also starved due to their quiescent state, the environmental temperature was the main external factor that distinguishes the seven-day development of groups b and c.

2.2. X-ray computer tomography

X-ray computer tomography (X-ray CT) scan of 42 animals (14 per group) was performed by using the Albira Si system (Bruker Corporation, Karksruhe, Germany), a trimodal PET/SPECT/CT scanner for small animal imaging. To immobilize the animals during the scan, they were anesthetized by isoflurane inhalation (Cooper, 2011). The Albira CT consists of an X-ray source and detector that are rotating around the subject in the step-and-shoot mode (source voltage 45 kV and source current 0.2 mA). We used its high-resolution setting, where 1000 projections are recorded, each with 2400 × 2400 pixels covering a 70 × 70 mm^2 field of view. The effective spatial resolution for this configuration

is 85 μm (Sánchez et al., 2013).

The resulting images were visualized with a medical data software (AMIDE, UCLA University. LA, USA). We have also used this software to select an ellipsoidal volume completely containing each individual and export the corresponding numerical data. These data consisted of the tomographic density expressed in Hounsfield units (UH) for each voxel. The voxel is the volume element of the 3D image and corresponds to a pixel in the 2D slice. The numerical data were subsequently analyzed through a commercial software, XLStat, which we also used for statistical studies (see subsection 2.5 below).

2.3. Digital holographic microscopy

Digital Holographic Microscopy (DHM) is an emerging technology that combines conventional microscopy with digital holographic processes (Rappaz et al., 2005). DHM uses a CCD camera to capture the interference of the wave coming from the object with a reference wave. From the resulting interference pattern, the software supplied with the system provides information from both phase and intensity of the object wave. This software also applies a phase unwrapping algorithm to reconstruct a three-dimensional image with information about the topology of the object surface (Kim, 2011). In this paper, we have used a DHM-R2100 (Lyncée Tec, Lausanne, Switzerland) holographic microscope (Cuche et al., 2009) with Koala software. The measurements were made with a lens 20x and wavelength of $\lambda = 684.9$ nm. This setup provides a horizontal resolution of 0.45 μm and a field area of 51.3 × 51.3 μm2. Height precision is 5 nm in the center of the image but degrades to 20 nm at the edges.

For DHM measurements, we used a scalpel to extract integument samples from anesthetized prepupae of the different groups and we immediately took their holographic images: 100 for each group. These images generally contained areas with different appearance and roughness. We then divided each image into 16 subzones (squares of 12.8 μm side). As an example, Fig. 1 shows the 3D profile of one of these subzones, where roughness appears as small-scale fluctuations around the average surface. For each subzone, we computed the integumental roughness as the maximum distance of its surface points to the local best-fit plane. The average roughness of a DHM image then corresponds to the average value of its 16 subzones.

2.4. Measurement of glucose in hemolymph

In order to quantify glucose as a potential cryoprotectant, we extracted hemolymph from all groups of larvae. Before collection, control and AT larvae were anesthetized for 1 min at −20 °C to immobilize them. Pre-pupae subjected to cold were in quiescence and hence it was not necessary to immobilize them.

Larvae integument was pierced by a needle and hemolymph of each individual was collected into 1.5 ml eppendorf tubes, centrifuged and stored at −80 °C until use.

The amount of glucose was determined spectrophotometrically using a Glucose Assay Kit (MAK263; Merck/Sigma-Aldrich), following the manufacturers' instructions (glucose detection ability 1–10,000 μM). Hemolymph samples were taken from 25, 29 and 23 control, cold and AT pre-pupae, respectively. Absorbance was measured at 570 nm for quantification (two replicates per individual).

2.5. Statistical analysis

Statistical analyses were performed with the XLStat software package (Addinsoft, New York, USA). For each type of data (volume percentage, roughness and glucose concentration), we tested the null hypothesis that the means of each pair of groups (control-cold, control-ambient temperature and cold-ambient temperature) correspond to the same distribution at a significance level of $P < 0.05$. To that end, we applied both the parametric one-way ANOVA and the non-parametric Mann-Whitney test. The latter does not require a normal distribution, checked in this paper through a battery of tests (Shapiro-Wilk, Anderson-Darling and Jarque-Bera tests), while the former requires normality, but it is quite robust against violation of this assumption. Although the null hypothesis of a normal or lognormal distribution was rejected for distributions of roughness, in all cases the one-way ANOVA and Mann-Whitney tests led to the same conclusions.

3. Results

3.1. Inner physiological features: X-Ray CT

Fig. 2 shows representative slices obtained with the Albira X-ray CT for each of the three groups of larvae. In this figure, the control and cold groups are represented by the same individual, scanned before and after cold treatment. The AT image corresponds instead to a different specimen. The color scale is the same in the three images and represents the tomographic density. We observe regions of moderately high tomographic density (yellow-red areas), which correspond to the cephalic capsule, cuticle and digestive tract. We also detect some internal organelles with moderately high tomographic density, but they represent a very small volume with respect to the total. The rest of the internal components is formed by the air contained in the tracheal structure (black areas) and low-density regions (green-blue areas), mainly fat body and hemolymph.

The comparison of the X-ray CT images shown in Fig. 2 is not direct, because they correspond to single slices extracted from three-dimensional (3D) images. The internal structures are 3D, so their

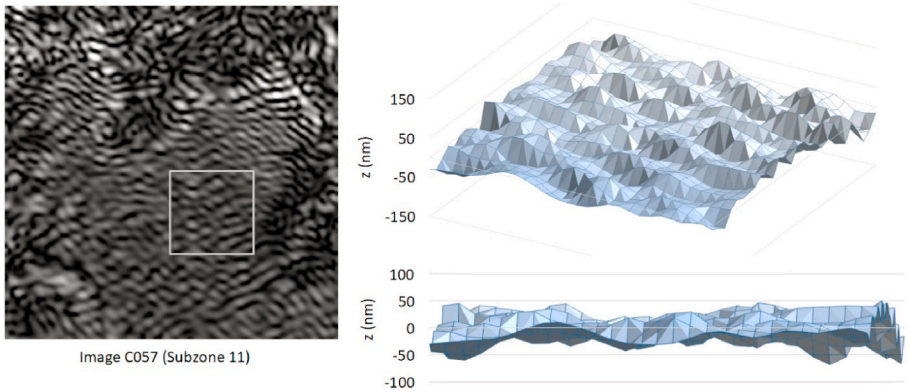

Fig. 1. Example of the roughness measurement. The left panel shows the image (intensity) of a sample and one of its subzones. For this selected subzone, the panels on the right show the 3D representation (top panel) obtained from the phase data, as well as its edge view (bottom panel). The integument roughness is the amplitude of fluctuations around the mean surface (best-fit plane).

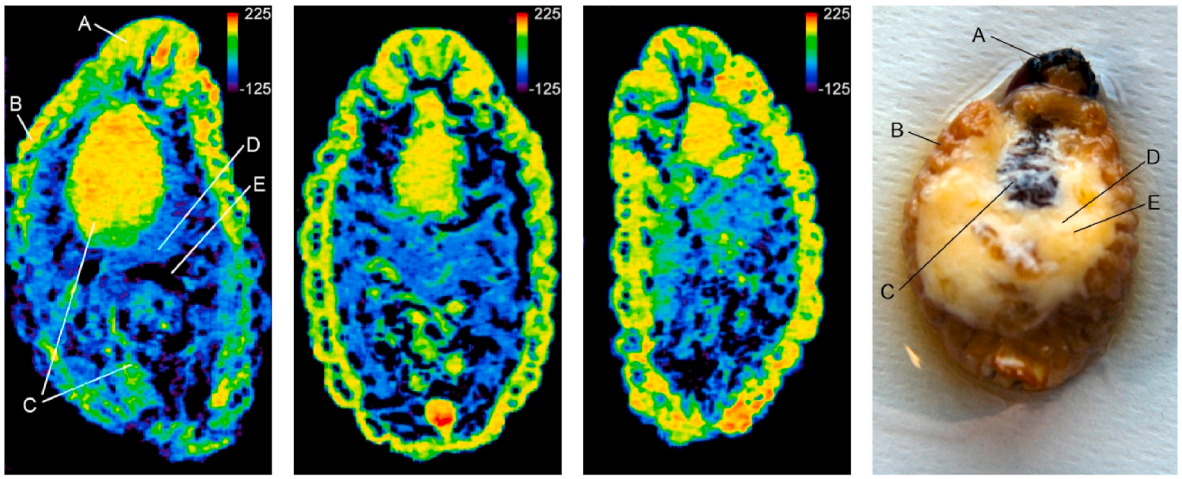

Fig. 2. X-ray CT slices of the three groups of larvae: (a) control, (b) cold and (c) ambient temperature. The scale of colors, from black to red, represents the tomographic density in Hounsfield units (UH). For comparison, (a) and (d) label the most quantitatively relevant morphological components: A. cephalic capsule, B. cuticle, C. digestive tract, D. fat body and E. tracheal structure (almost translucent and mixed with the fat).

apparent shape depends on the depth to which the 2D slice was extracted. Nevertheless, the inspection of Fig. 2 and other alternative slices already shows that individuals subjected to both cold and ambient temperature seem to have developed an external cuticle thicker and denser than in the initial control state. Therefore, the proportion between low and moderately high dense tissues seems to be different in the three groups of larvae. In order to quantify the percentage of the different tissues, as well as the possible differences between groups of animals, we analyzed the distribution of tomographic densities in each individual introduced into the X-ray CT system. The histograms in Fig. 3 show the number of voxels (proportional to volume) as a function of tomographic density in three representative cases, one for each group. In the 42 individuals analyzed, without exception, the histograms consisted of different zones always separated by the same tomographic density values.

Low-density zones (from −200 to 60 UH). At a tomographic density of $\rho_{min} = -200$ UH, all distributions present a sudden jump in the frequency of voxels. This step corresponds to the separation between the external background (air with a certain relative humidity) and the less dense tissues of the animal. In addition, we also observe another step at $\rho_{border} = 60$ UH, which evidences the separation between two different types of tissues.

Within this low-density region (from $\rho = -200$ to 60 UH), we also observe a subregion (from $\rho = -32$ to 0 UH) with a peak that rises above the general distribution. The analysis of the X-ray CT images (see Fig. 4a) shows that such a peak corresponds to hemolymph, while the background distribution essentially corresponds to fat.

Border (from 60 to 120 UH) and moderately high-density (>120 UH) zones. For tomographic densities above 60 UH, we find two clearly distinct subzones. First, a region of very small volume (low number of voxels) with densities between 60 and 120 UH. In the X-ray CT images (Fig. 4b), this region appears as the boundary that separates areas of low and moderate density. The other subzone begins with a sharp increase in the number of voxels at $\rho = 120$ UH, and then decays to practically zero for $\rho > 224$ UH. This subzone corresponds to the densest tissues of the animal (cuticle and cephalic capsule), but also to the content of the digestive tract, quite opaque to X-rays.

Once identified the minimum (ρ_{min}) and maximum (ρ_{max}) tomographic density of each internal component of animals, the volume of the different components can be computed by integrating the distribution of ρ between the corresponding values of ρ_{min} and ρ_{max}. In the same way, the integral between the extreme values of ρ (−200 and 224 UH) gives the total volume of the animal excluding air in internal cavities. This in turn provides the percentage in volume represented by each component.

Data are average values ± S.E.M. Within columns, values with different superscripts (a, b) are significantly different at $P < 0.05$. Dense Tissue (D.T.) includes cuticle, cephalic capsule and digestive tract.

Table 1 summarizes our results for the volume percentage of the different components, or density zones, in the three groups of larvae. To separate the contribution of hemolymph and fat body, which overlap in the range $-32 < \rho < 0$ UH, we have fitted the background fat body distribution to a cubic polynomial, which subtracted from the total gives a good approximation of the relative volume of hemolymph. These results are also shown in Fig. 5, which displays the average composition in hemolymph, fat body and moderately dense zones (tissues and border) for the three groups of samples.

3.2. Outer physiological features: digital holographic microscopy

Fig. 6 displays the results obtained from digital holographic microscopy for the frequency distribution of the cuticle roughness in the three groups of samples. All groups have the same number of data (1600 subzones in 100 DHM images). We see that the roughness distributions have quite different shapes and a wide dispersion of data, with mean values of 0.15 ± 0.09 μm (control), 0.12 ± 0.09 μm (cold) and 0.10 ± 0.09 μm (AT). Statistical tests rejected the hypothesis of normal (and lognormal) distributions. In addition, these tests conclude that all distributions are significantly different at $P < 0.05$. Indeed, they differ in the height of the maximum and in the subsequent rate of decrease. The control group has a smooth secondary maximum at roughness of about 0.18 μm. The cumulative frequency (fourth panel of Fig. 6) indicates that 50% of the control samples (solid lines) have roughness above 0.15 μm. At the opposite extreme, the ambient temperature group (dotted line) has a very pronounced maximum at low roughness and then the distribution falls very abruptly. The cumulative frequency indicates that 80% of the samples from this group have roughness less than 0.15 μm. The cold group (dashed line) is intermediate between the two previous ones, with 65% of samples with roughness less than 0.15 μm. The averaging over 1600 subzones or 100 images leads to the same conclusions.

3.3. Cryoprotective response

Figs. 7 and 8 show the results concerning glucose level in

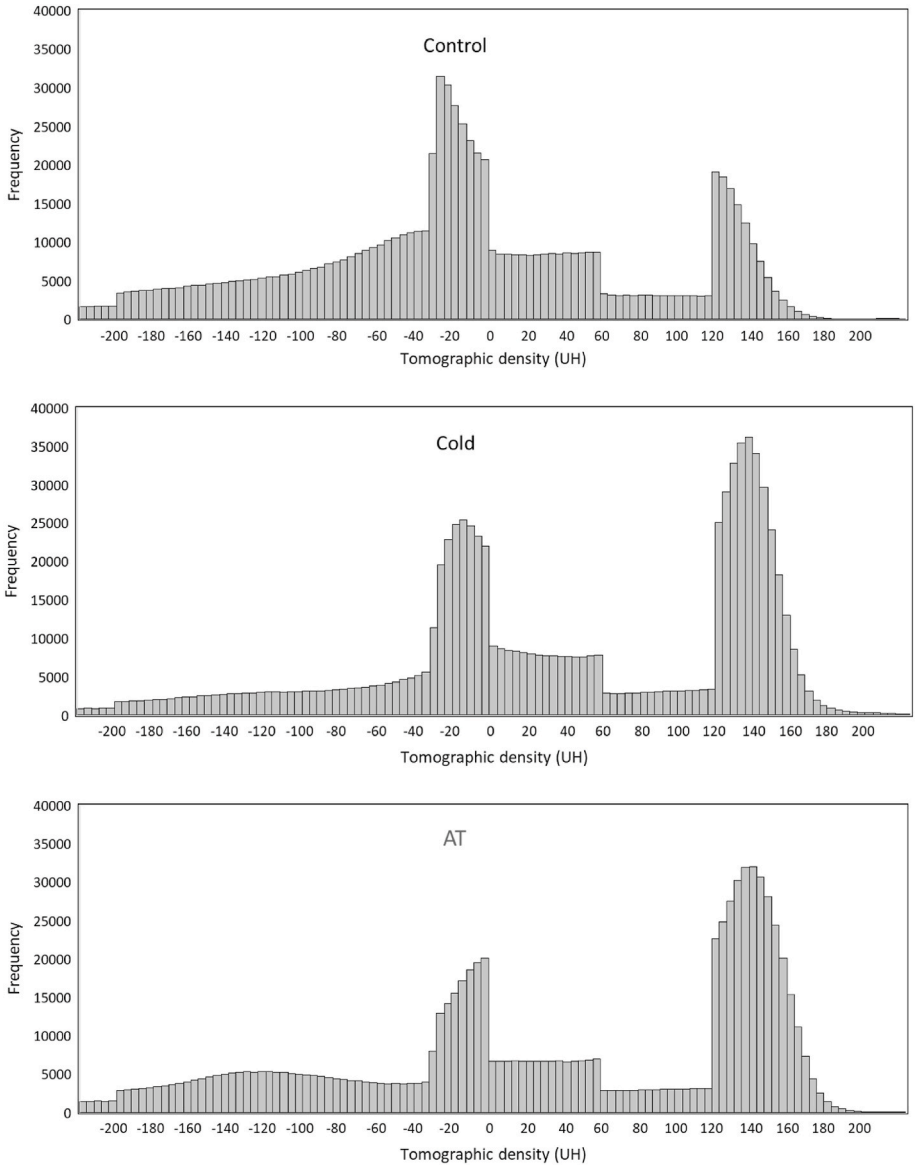

Fig. 3. Typical distribution of the tomographic density in each of the three groups of larvae: controls, subjected to cold and ambient temperature (AT).

hemolymph. We see from these figures that larvae that remained for 7 day at ambient temperature (AT) have slightly lower glucose concentration than those presented by the control ones, although the difference is not statistically significant (0.8 ± 0.2 vs. 1.0 ± 0.4 mmol/L, respectively). For both control and AT groups, glucose values are always less than 2.3 mmol/L (left panel in Fig. 7) and their cumulative frequency profiles practically overlap (Fig. 8). However, a large part of the larvae exposed to cold stress for 7 days presented glucose concentration considerably higher than in the other two groups, with an average value of 5.8 mmol/L and a maximum peak of 17.5 mmol/L (Fig. 7). In the same way, the cumulative frequency profile is clearly different from those found for groups not subjected to cold (Fig. 8).

Nevertheless, cold treated individuals have an unequal response. When looking at the left panel of Fig. 7, glucose concentration in response to cold seems to divide larvae into two subpopulations. Almost half (48.3%) of the larval population subjected to cold did not show an increase in their glucose level, which was similar (0.6–2.5 mmol/L) to those observed both in the control and AT groups. In contrast, the remaining subpopulation (51.7%) responded to cold by increasing glucose concentration, although in a heterogeneous way, with values ranging from 4.0 to 17.5 mmol/L.

4. Discussion

In this work, we used an imaging technique, X-Ray Computer Tomography, which in recent years has allowed new insights into tissue morphology and internal anatomy of different animal species (e.g., Smith et al., 2016). Our study has focused on the internal and external morphological response of the RPW to a sudden but transient decrease in the environmental temperature. By graphical analysis of CT data, different authors (e.g., Smith et al., 2016) have reported precise volumetric estimates of different internal organs in insects. The volume of hemolymph is however difficult to quantify since insects have an open circulatory system. In this work, we have accurately measured the volumes of hemolymph, fat body and other tissues, as well as their changes under different environmental temperatures.

From the distribution of tomographic densities, we have found that control RPW larvae have a fat body content of 58% by volume. This value is in close agreement with that found (57–60% by weight) for the RPW from a completely different methodology (Cito et al., 2017). We find that, after 7 days, pre-pupae from both cold and AT groups significantly separate from controls and follow a development in which their fat body content decreases while a thick and dense cuticle forms. A

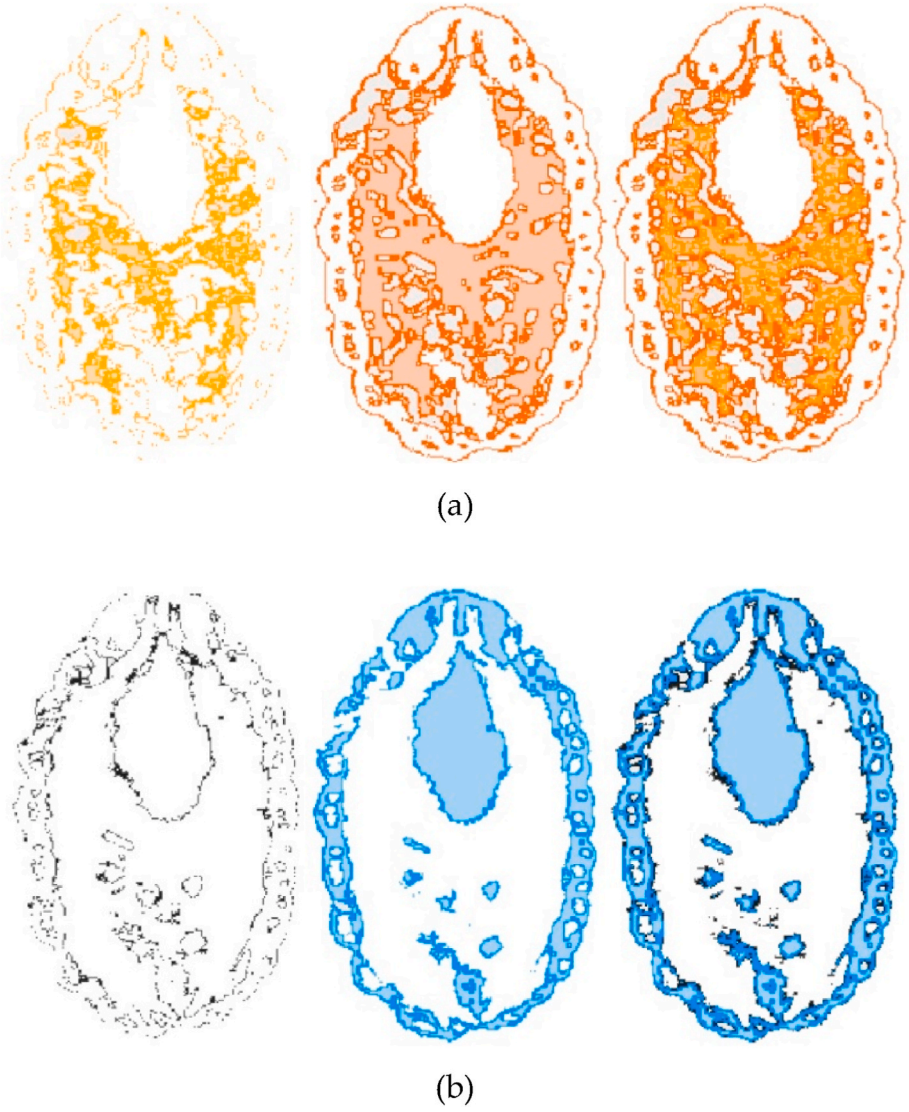

Fig. 4. Identification of areas with different tomographic densities: a) Low-density zones. From left to right: mainly hemolymph ($-32 \leq \rho \leq 0$ UH), fat body (remaining voxels with $-200 \leq \rho \leq 60$ UH) and sum of both; b) Moderate-density zones: from left to right: border ($60 \leq \rho \leq 120$ UH), dense tissues ($\rho > 120$ UH) and sum of both.

Table 1
Volume percentage of different tissues in the three groups of larvae.

Group	Low density zones (%)			Moderate-density zones (%)			Fat/D.T. ratio
	Fat body	Hemolymph	Total	Dense Tissue	Border	Total	
Control	58 ± 3^a	15 ± 1^a	73 ± 3^a	20 ± 3^a	7 ± 1^a	27 ± 3^a	3.0 ± 0.6^a
Cold	42 ± 3^b	14 ± 2^a	56 ± 3^b	38 ± 3^b	5 ± 1^b	44 ± 3^b	1.1 ± 0.2^b
Ambient	43 ± 3^b	11 ± 2^b	54 ± 4^b	39 ± 4^b	7 ± 2^a	46 ± 4^b	1.1 ± 0.2^b

possible explanation for these changes is the fat body and cuticle remodeling during the larva-pupal transition. Indeed, in holometabolous insects, the fat body synthesizes and stores proteins that participate during pupation in the development of tissues such as the cuticle (Csikós et al., 1999; Gullan and Cranston, 2010), which in some species becomes thicker than in larval stages (Moussian, 2010). In addition, during the larva-pupal transition, the fat body is used as the main energy source (Nestel et al., 2003). The higher energy requirement and the feeding cessation in this stage would cause the progressive consumption of this energy reserve. Our X-Ray CT results for cold and AT groups then reveal that a decrease in the environmental temperature for seven days has not stopped the RPW larval-pupal transition. Only some aspects seem to indicate a slight delay in the rate of development of pre-pupae subjected to low temperatures. This is the case of the hemolymph content, which is similar in the control (15%) and cold (14%) groups, while it is slightly but significantly smaller (11%) in the ambient temperature group.

The results obtained from digital holographic microscopy also show morphological changes in the integument shape' architecture of animals subjected for seven days to a low temperature (cold group) and animals that remained the same time at room temperature (AT group). In both cases, the integument has followed during this time a development in which the roughness of its outer surface decreases. More precisely, there is a higher percentage of integumental areas with low roughness. Compared to the initial control state, these differences in roughness are

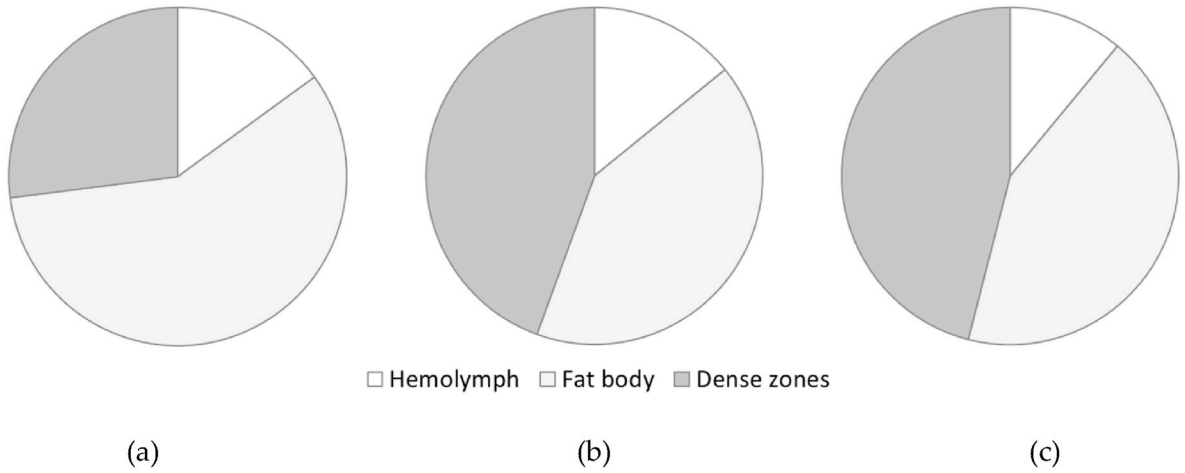

Fig. 5. Average composition in hemolymph (white), fat body (light grey) and dense zones (dark grey) in (a) control, (b) cold and (c) ambient temperature groups.

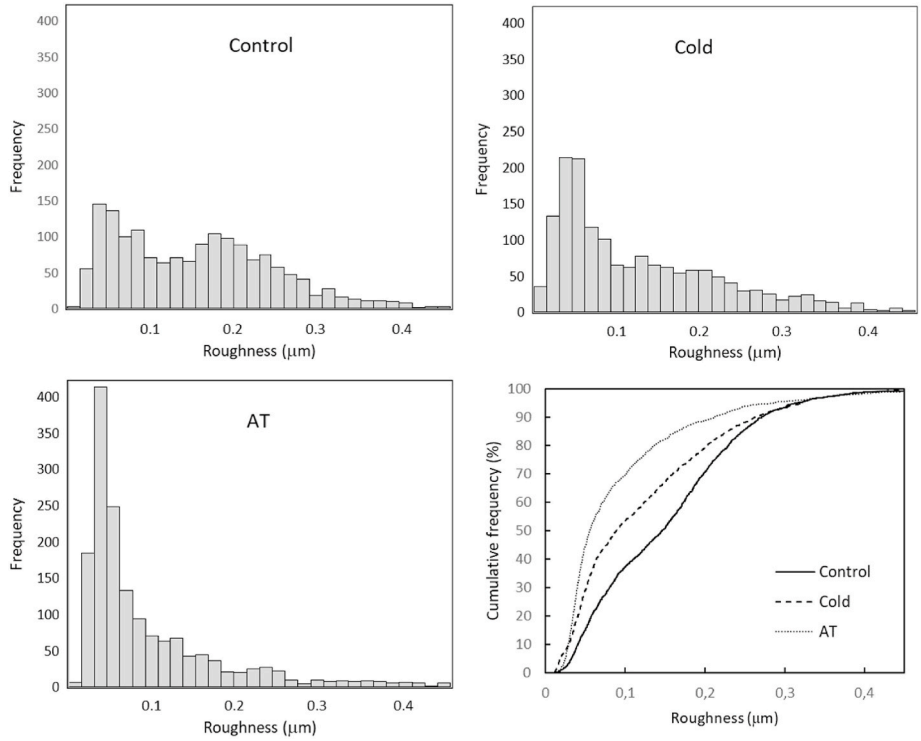

Fig. 6. Distribution and cumulative frequency of the cuticle roughness in the three types of samples: controls, subjected to cold and ambient temperature (AT).

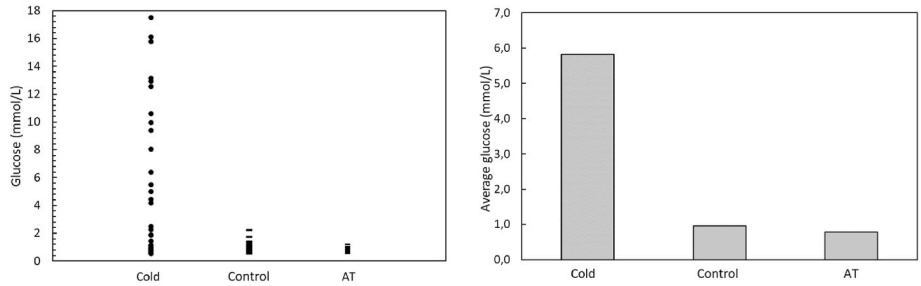

Fig. 7. Individual (left panel) and average (right panel) values of hemolymph glucose concentration (mmol/L) in the three groups of Red Palm Weevil pre-pupae: controls, subjected to cold and ambient temperature (AT).

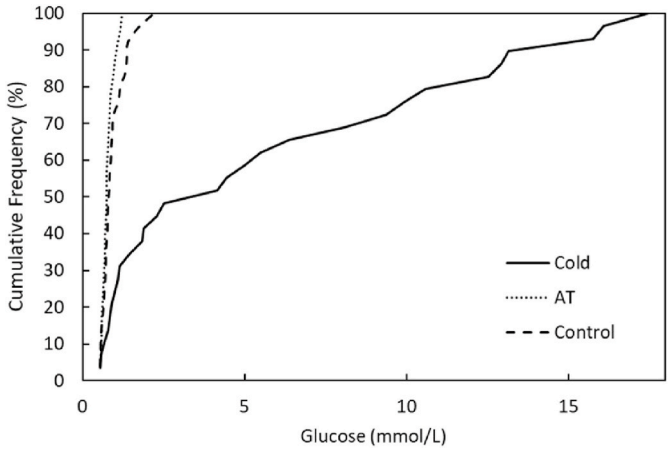

Fig. 8. Cumulative frequency of glucose values (mmol/L) from Red Palm Weevil larvae at prepupal stage in the three groups analyzed.

significant for both cold and AT samples. We thus obtain again that RPW pre-pupae subjected to a low temperature have not experienced a stop in their development. However, a more obvious developmental delay is now observed in the results obtained by holographic microscopy, with the cold group appearing as a significantly different and intermediate state between the control and AT groups.

Regarding the hemolymph glucose level, we find that over half (51.7%) of pre-pupae subjected to cold presented an increase of glucose concentration up to an average value six times greater than in groups with no cold stress (controls and AT). These values are similar, in absolute terms (from about 1 to 6 mmol/L), to those previously found by other authors for some overwintering Coleoptera (Feng et al., 2016), where glucose was identified among other cryoprotectant substances. In relative terms, a 6-fold increase is also comparable to the glucose increase found in the literature for different insects living in cold zones. For example, the 6-fold increase found by Saeidi and Moharramipour (2017) or the 3-fold found by Shao et al. (2018). Similarly, WangQi and Kang (2010) and Chowanski et al. (2015) have reported in tropical species a glucose increase of 6-fold and 2-fold, respectively. Our results then suggest a physiological role of glucose as one of the endogenous cryoprotectants used by RPW pre-pupae to deal with and overcome a sudden and transient low temperature event.

Additionally, our results of 51.7% of pre-pupae that increased their glucose level roughly coincides with the final survival rate of 60% previously found by Martin and Cabello (2005, 2006) for RPW pupae subjected to the same conditions (7 days at 5 °C) as in the present work. Taking all these results together, we hypothesize a possible link between the observed survival rate and the percentage of individuals that developed a cryoprotective response, where glucose seems to play a significant role, very likely in combination with other substances.

5. Summary and conclusions

In this work, we have studied the morphological response of the RPW to a sudden and transitory decrease in the environmental temperature. More specifically, we have analyzed whether such a morphological response shows evidence of an arrest or some delay in the RPW development. The approach that we have followed has several innovative aspects. On the one hand, we have used a modern noninvasive imaging technique, X-Ray Computer Tomography, where we have developed a procedure to carry out fast and automated measurements of the volumetric content of hemolymph, fat body and other tissues. On the other hand, we make use of another emerging technique, Digital Holographic Microscopy (DHM). As far as we know, this is the first time that DHM has been used to quantify the roughness of insect tissues.

Our results provide morphological evidence that the larval-pupal transition of the RPW continues almost undisturbed even during the quiescence induced by cold stress. Indeed, both pre-pupae subjected to cold and those remaining in optimal environmental temperature followed a seven-day development in which their fat body content decreases while a thick and dense cuticle is formed. Such a development and the rate of change of fat body and dense tissues resulted to be indistinguishable between both groups. Nevertheless, the decrease in the volume of hemolymph, as well as in the cuticle roughness, indicate a slight delay in the development of individuals subjected to cold treatment.

We also show for the first time the ability of the RPW, a species native to warm places, to increase the secretion of certain substances to deal with cold temperatures. In this work, we have analyzed glucose as one of the potentially cryoprotective substances. Our results suggest a physiological role of glucose as one of the endogenous cryoprotectants used by RPW pre-pupae as part of their cold tolerance strategy. Very likely, other substances (e.g. trehalose, glycerol …) could also play a major role within this cold resistance strategy. A detailed analysis of all these substances will be addressed in a future work.

Finally, our results can be relevant to deepen the knowledge of cold adaptation in insects inhabiting warm geographical areas, especially under a context of climatic unpredictability. In addition, the knowledge of the physiological bases underlying the adaptive responses of pest insects could be relevant to better design strategies to combat them.

Author contributions

TLQ and AS conceived the ideas, designed the experiments, carried out the X-Ray CT and glucose measurements, analyzed and interpreted all results and drafted the original manuscript. AF and RM designed and collected the DHM measurements and provided feedbacks on their interpretation. All authors have read the manuscript and approved its final version.

Funding

León-Quinto and Serna thank financial support through the project PAR UMH-2018, Universidad Miguel Hernández, Elche, Spain.

Conflicts of Interest

The authors declare no conflict of interest.

CRediT authorship contribution statement

Trinidad León-Quinto: Conceptualization, Methodology, Data curation, Writing - original draft, Supervision, Investigation, Funding acquisition. **Antonio Fimia:** Data curation, DHM, Investigation. **Roque Madrigal:** Data curation, DHM, Investigation. **Arturo Serna:** Conceptualization, Methodology, Data curation, Writing - original draft, Supervision, Investigation.

Acknowledgments

Special thanks to Victoria Martinez Bas and Jose Juan Lopez Calatayud from the public company TRAGSA for providing us with red palm weevil specimens. We are indebted to them for their great support and enthusiasm in helping us.

References

Bathiany, S., Dakos, V., Scheffer, M., Lenton, T.M., 2018. Climate models predict increasing temperature variability in poor countries. Science Advances 4, 1–10.

Cabello, T., 2006. Population biology and dynamics of the red palm weevil, Rhynchophorus ferrugineurs. In: I Jornada Internacional sobre el Picudo Rojo de las Palmeras. Conselleria de Agricultura, Pesca y alimentación, Valencia, Spain, ISBN 84-690-1742-X, pp. 19–34.

Cito, A., Longo, S., Mazza, G., Dreassi, E., Francardi, V., 2017. Chemical evaluation of the Rhynchophorus ferrugineus larvae fed on different substrates as human food source. Food Sci. Technol. Int. 23, 529–539.
Chowanski, S., Lubawy, J., Spochacz, M., Ewelina, P., Grzegorz, S., Rosinski, G., Slocinska, M., 2015. Cold induced changes in lipid, protein and carbohydrate levels in the tropical insect Gromphadorhina coquereliana. Comp. Biochem. Physiol. Mol. Integr. Physiol. (183), 57–63.
Cooper, J.E., 2011. Anesthesia, analgesia, and euthanasia of invertebrates. ILAR J. 52, 196–204.
Csikós, G., Molnár, K., Borhegyi, N.H., Talián, G.C., Sass, M., 1999. Insect cuticle, an in vivo model of protein trafficking. J. Cell Sci. 112, 2113–2124.
Cubillos, C., Cáceres, J.C., Villablanca, C., Villarreal, P., Baeza, M., Cabrera, R., Graether, P., Veloso, C., 2018. Cold tolerance mechanisms of two arthropods from the andean range of Central Chile: agathemera crassa (insecta: agathemeridae) and euathlus condorito (arachnida: theraphosidae). J. Therm. Biol. 74, 133–139.
Cuche, E., Emery, Y., Montfort, F., 2009. One-shot analysis. Nat. Photon. 3 (11), 633–635.
Dembilio, O., Jacas, J.A., 2011. Basic bio-ecological parameters of the invasive Red Palm Weevil, Rhynchophorus ferrugineus (Coleoptera: Curculionidae), in Phoenix canariensis under Mediterranean climate. Bull. Entomol. Res. 101, 153–163.
Denlinger, D.L., Lee, R.E., 2010. Low Temperature Biology of Insects. Cambridge University Press.
Durak, R., Dampc, J., Dampc, J., Bartoszewski, S., Michalik, A., 2020. Uninterrupted development of two aphid species belonging to Cinara genus during winter diapause. Insects 11 (3), 150.
Feng, Y., Xu, L., Li, W., Xu, Z., Cao, M., Wang, J., Tao, J., Xong, S., 2016. Seasonal changes in supercooling capacity and major cryoprotectants of overwintering Asian longhorned beetle (Anoplophora glabripennis) larvae. Agric. For. Entomol. 18, 302–312.
Gu, L., Hanson, P.J., Mac Post, W., Kaiser, D.P., Yang, B., Nemani, R., Pallardy, S.G., Meyers, T., 2008. The 2007 eastern US spring freeze: increased cold damage in a warming World? Bioscience 58, 253–262.
Gullan, P.J., Cranston, P.S., 2010. The Insects. An Outline of Entomology, fourth ed. Wiley-Blackwell, pp. 80–81.
Gutiérrez, Y., Ott, D., Töpperwien, M., Salditt, T., Scherber, S., 2018. X-ray computed tomography and its potential in ecological research: a review of studies and optimization of specimen preparation. Ecology and Evolution 8, 7717–7732.
Hansen, J., Sato, M., Ruedy, R., 2012. Perception of climate change. Proc. Natl. Acad. Sci. Unit. States Am. 109, E2415–E2423.
Kim, M.K., 2011. Digital Holographic Microscopy: Principles, Techniques, and Applications. Springer, New York.
Koštál, V., Korbelová, J., Štětina, T., Poupardin, R., Colinet, H., Zahradníčková, H., Opekarová, I., Moos, M., Šimek, P., 2016. Physiological basis for low temperature survival and storage of quiescent larvae of the fruit fly Drosophila melanogaster. Sci. Rep. 6 (32346), 1–11.
Koštál, V., Korbelová, J., Štětina, T., Poupardin, R., Korbelová, J., Bruce, A.W., 2017. Conceptual framework of the eco-physiological phases of insect diapause development justified by transcriptomic profiling. Proc. Natl. Acad. Sci. Unit. States Am. 114, 8532–8537.
Lencioni, V., 2004. Survival strategies of freshwater insects in cold environments. J. Limnol. 63 (Suppl. 1), 45–55.
Martin, M.M., Cabello, T., 2005. Biología y ecología del curculiónido rojo de la palmera, Rhynchophorus ferrugineus. Universidad de Almería, Spain, ISBN 84-689-5292-3, pp. 1–202.
Martin, M.M., Cabello, T., 2006. In: Manejo de la cría del picudo rojo de la palmera, Rhynchophorus ferrugineus (Olivier, 1790) (Coleoptera, Dryophthoridae), en dieta artificial y efectos en su biometría y biología, vol. 32. Boletín de Sanidad Vegetal de Plagas, pp. 631–641.
Michaud, M.R., Denlinger, D.L., 2007. Shifts in the carbohydrate, polyol, and amino acid pools during rapid cold-hardening and diapause-associated cold-hardening in flesh flies (Sarcophaga crassipalpis): a metabolomic comparison. J. Comp. Physiol. B 177, 753–763.
Moussian, B., 2010. Recent advances in understanding mechanisms of insect cuticle differentiation. Insect Biochem. Mol. Biol. 40 (5), 363–375.
Nation, J.L, 2008. Insect Physiology and Biochemistry, 2nd Edition. CRC Press, pp. 161–175.
Nestel, D., Tolmasky, D., Rabossi, A., Quesada-Allué, L.A., 2003. Lipid, carbohydrates and protein patterns during metamorphosis of the mediterranean fruit fly, ceratitis capitate (Diptera: tephritidae). Ann. Entomol. Soc. Am. 96, 237–244.
Overgaard, J., Malmendal, A., Sørensen, J.G., Bundy, J.G., Loeschcke, V., Nielsen, N.C., Holmstrup, M., 2007. Metabolomic profiling of rapid cold hardening and cold shock in Drosophila melanogaster. J. Insect Physiol. 53, 1218–1232.
Rappaz, B., Marquet, P., Cuche, E., Emery, Y., Depeursinge, C., Magistretti, P.J., 2005. Measurement of the integral refractive index and dynamic cell morphometry of living cells with digital holographic microscopy. Optic Express 13 (23), 9361–9373.
Rugman-Jones, P.F., Hoddle, C.D., Hoddle, M.S., Stouthamer, R., 2013. The lesser of two weevils: molecular-genetics of pest palm weevil populations confirm Rhynchophorus vulneratus (panzer 1798) as a valid species distinct from R. Ferrugineus (olivier 1790), and reveal the global extent of both. PloS One 8 (10), e78379.
Saeidi, M., Moharramipour, S., 2017. Physiology of cold hardiness, seasonal fluctuations, and cryoprotectant contents in overwintering adults of hypera postica (Coleoptera: Curculionidae). Environ. Entomol. 46 (4), 960–966.
Sánchez, F., Orero, A., Soriano, A., Correcher, C., Conde, P., González, A., Hernández, L., Moliner, L., Rodríguez-Alvarez, M.J., Vidal, L.F., Benlloch, J.M., Chapman, S.E., Leevy, W.M., 2013. ALBIRA: a small animal PET/SPECT/CT imaging system. Med. Phys. 40, 1–11.
Shao, Y., Feng, Y., Tian, B., Wang, T., He, Y., Zong, S., 2018. Cold hardiness of larvae of Dendrolimus tabulaeformis (Lepidoptera: Lasiocampidae) at different stages during the overwintering period. Eur. J. Entomol. 115, 198–207.
Smith, D.B., Bernhardt, G., Raine, N.E., Abel, R.L., Sykes, D., Ahmed, F., Pedroso, I., Gill, R.J., 2016. Exploring miniature insect brains using micro-CT scanning techniques. Sci. Rep. 6, 21768.
Storey, K.B., 1997. Organic solutes in freezing tolerance. Comp. Biochem. Physiol. Physiol. 117, 319–326.
Storey, K.B., Storey, J.M., 1988. Freeze tolerance in animals. Physiol. Rev. 68, 27–84.
Stouffer, R.J., Wetherald, R.T., 2007. Changes of variability in response to increasing greenhouse gases. Part I: Temperature. J. Clim. 20, 5455–5467.
Teets, N.M., Delinger, D.L., 2013. Physiological mechanisms of seasonal and rapid cold-hardening in insects. Physiol. Entomol. 38, 105–116.
Toxopeus, J., Sinclair, B., 2018. Mechanisms underlying insect freeze tolerance. Biol. Rev. 93, 1891–1914.
Toxopeus, J., Koštál, V., Sinclair, B.J., 2019. Evidence for non-colligative function of small cryoprotectants in a freeze-tolerant insect. Proceedings of the Royal Society B 286 (1899), 20190050.
Valenzuela, N., Literman, R., Neuwald, J.K., Mizoguchi, B., Iverson, J.B., Riley, J.L., Litzgus, J.D., 2019. Extreme thermal fluctuations from climate change unexpectedly accelerate demographic collapse of vertebrates with temperature-dependent sex determination. Sci. Rep. 9 (4254), 1–11.
Wang, X.H., Qi, X.L., Kang, L., 2010. Geographic differences on accumulation of sugars and polyols in locust eggs in response to cold acclimation. J. Insect Physiol. 56, 966–970.